Measurement of $e^+e^- \to \gamma\chi_{cJ}$ via ISR at Belle Experiment

Yanliang Han

Shandong University

June 11, 2015

Motivation

- The potential models predict five vector states

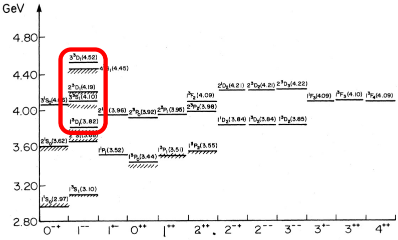

Figure: The charmonium $c\bar{c}$ [1]

[1] S. Godfrey and N. Isgur, Phys. Rev. D **32**, 189 (1985)

Motivation

- The potential models predict five vector states
- Six vector states are discovered at Experiments.

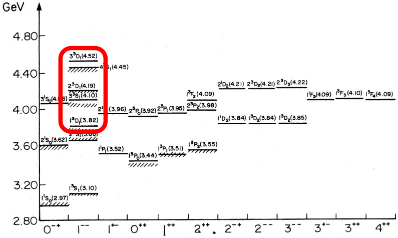

Figure: The charmonium $c\bar{c}$ [1]

[1] S. Godfrey and N. Isgur, Phys. Rev. D **32**, 189 (1985)

Motivation

- The potential models predict five vector states

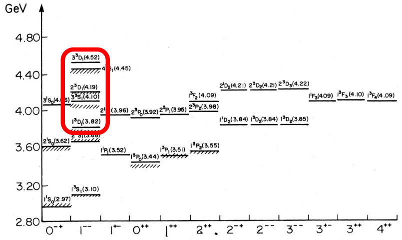

Figure: The charmonium $c\bar{c}$ [1]

[1] S. Godfrey and N. Isgur, Phys. Rev. D **32**, 189 (1985)

- Six vector states are discovered at Experiments.
- The conventional $\psi(4040)$, $\psi(4160)$ and $\psi(4415)$

Motivation

- The potential models predict five vector states

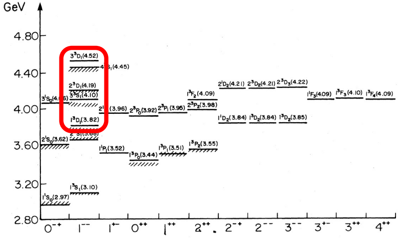

Figure: The charmonium $c\bar{c}$ [1]

- Six vector states are discovered at Experiments.
- The conventional $\psi(4040)$, $\psi(4160)$ and $\psi(4415)$

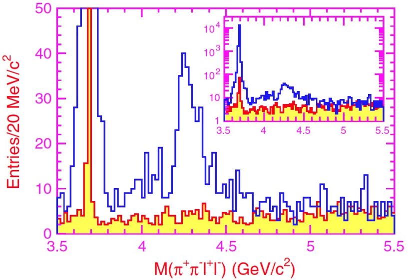

Figure: Invariant mass of $\pi^+\pi^- J/\psi$, Y(4260) [2]

[1] S. Godfrey and N. Isgur, Phys. Rev. D **32**, 189 (1985)
[2] C. Z. Yuan *et al.* (Belle Collaboration),Phys. Rev. Lett. **99**, 182004 (2007)

Motivation

- The potential models predict five vector states

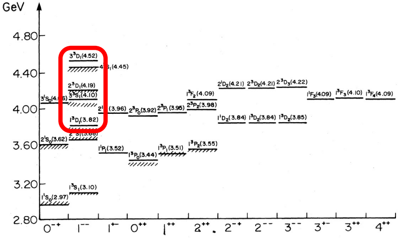

Figure: The charmonium $c\bar{c}$ [1]

[1] S. Godfrey and N. Isgur, Phys. Rev. D **32**, 189 (1985)
[3] X. L. Wang *et al.* (Belle Collaboration),Phys. Rev. Lett. **99**, 142002 (2007)

- Six vector states are discovered at Experiments.
- The conventional $\psi(4040)$, $\psi(4160)$ and $\psi(4415)$

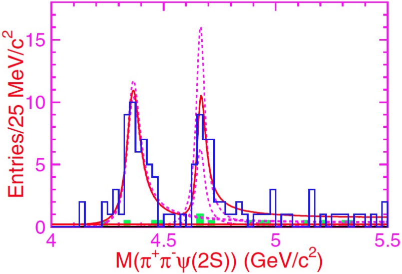

Figure: Invariant mass of $\pi^+\pi^-\psi(2S)$, Y(4360) Y(4660) [3]

Motivation

- The potential models predict five vector states
- Six vector states are discovered at Experiments.

Some of these states show unusual properties: Maybe exotic states.

Motivation

- The potential models predict five vector states
- Six vector states are discovered at Experiments.

Some of these states show unusual properties: Maybe exotic states.

- Y(4260),Y(4360) did not show up in hadronic R inclusive scan

Motivation

- The potential models predict five vector states
- Six vector states are discovered at Experiments.

Some of these states show unusual properties: Maybe exotic states.

- Y(4260),Y(4360) did not show up in hadronic R inclusive scan
- Large dipion transitions rate than conventional charmonium.

Motivation

- The potential models predict five vector states
- Six vector states are discovered at Experiments.

Some of these states show unusual properties: Maybe exotic states.

- Y(4260),Y(4360) did not show up in hadronic R inclusive scan
- Large dipion transitions rate than conventional charmonium.

It is important to investigate them using much larger data samples and new decay channels.

Motivation

- The potential models predict five vector states
- Six vector states are discovered at Experiments.

Some of these states show unusual properties: Maybe exotic states.

- Y(4260),Y(4360) did not show up in hadronic R inclusive scan
- Large dipion transitions rate than conventional charmonium.

It is important to investigate them using much larger data samples and new decay channels.

- Full Belle data sample

Motivation

- The potential models predict five vector states
- Six vector states are discovered at Experiments.

Some of these states show unusual properties: Maybe exotic states.

- Y(4260),Y(4360) did not show up in hadronic R inclusive scan
- Large dipion transitions rate than conventional charmonium.

It is important to investigate them using much larger data samples and new decay channels.

- Full Belle data sample
- Radiative transitions: $e^+e^- \to \gamma\chi_{cJ}$ via ISR, $\chi_{cJ} \to \gamma J/\psi$, $J/\psi \to \mu^+\mu^-$

Data and MC Samples

DATA

- Full Belle data sample, integrated luminosity is 980 fb^{-1}.

MC Samples

- EVTGEN with the VECTORISR model is used to simulate the signal process $e^{+}e^{-} \to \gamma_{\mathrm{ISR}} V \to \gamma_{\mathrm{ISR}}\gamma\chi_{cJ} \to \gamma_{\mathrm{ISR}}\gamma\gamma J/\psi$
- Background MC samples are generated with PHOKHARA

Event selection

- Two good charged tracks with zero net charge

Event selection

- Two good charged tracks with zero net charge
- Muon identification is required

Event selection

- Two good charged tracks with zero net charge
- Muon identification is required
- Two highest energy photons (Non ISR) in the lab. system

Event selection

- Two good charged tracks with zero net charge
- Muon identification is required
- Two highest energy photons (Non ISR) in the lab. system
- Reject $\eta(\pi^0)J/\psi$ events
  - $M(\gamma\gamma)$ are not in the η mass region $[0.50,\ 0.58]\ \mathrm{GeV}/c^2$
  - $M(\gamma\gamma) > 0.20\ \mathrm{GeV}/c^2$ to reject π^0 and other low invariant mass events

Missing Mass Square

Defined as $M^2_{\rm rec} = (P_{e^+e^-} - P_{\gamma\gamma\mu^+\mu^-})^2$

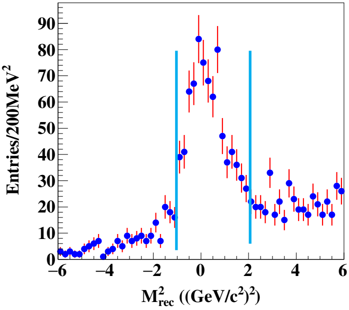

Figure: MMS distribution with $M(\gamma_l\gamma_h J/\psi) < 5.56$ GeV$/c^2$

Here $M(\gamma_l\gamma_h J/\psi) = M(\gamma_l\gamma_h\mu^+\mu^-) - M(\mu^+\mu^-) + m_{J/\psi}$

We require: $-1\ (\mathrm{GeV}/c^2)^2 < M^2_{\rm rec} < 2\ (\mathrm{GeV}/c^2)^2$

Invariant mass of $\mu^+\mu^-$

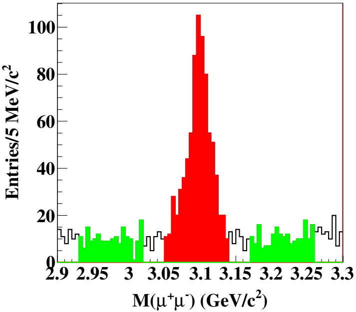

Figure: Invariant mass distribution of $\mu^+\mu^-$. The shaded area in the middle is the J/ψ signal region, and the shaded regions on both sides are the J/ψ mass sidebands.

- J/ψ signal region: Within $\pm 45\ \mathrm{MeV}/c^2$ of the J/ψ mass
- J/ψ sideband: $[3.172,\ 3.262]$ or $[2.932,\ 3.022]\ \mathrm{GeV}/c^2$

Invariant mass of $\gamma J/\psi$

Including $M(\gamma_h J/\psi)$ and $M(\gamma_l J/\psi)$, two entries per event

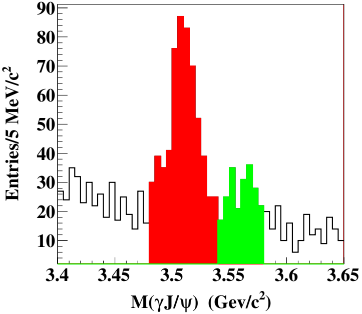

Figure: Invariant mass distribution of $\gamma J/\psi$ for candidate events with $M(\gamma_l \gamma_h J/\psi) < 5.56$ GeV/c^2. The shaded histograms show the χ_{c1} ($[3.48, 3.535]$ GeV/c^2) and χ_{c2} ($[3.535, 3.58]$ GeV/c^2) regions.

Potential background

- Non J/ψ background. This can be estimated by J/ψ sideband

Potential background

- Non J/ψ background. This can be estimated by J/ψ sideband
- $e^+e^- \to \gamma_{\rm ISR} J/\psi$
  - This cross section can be calculated theoretically

Potential background

- Non J/ψ background. This can be estimated by J/ψ sideband
- $e^+e^- \to \gamma_{\mathrm{ISR}} J/\psi$
  - This cross section can be calculated theoretically
- $e^+e^- \to \gamma_{\mathrm{ISR}} \pi^0\pi^0 J/\psi$
  - $\sigma(e^+e^- \to \pi^0\pi^0 J/\psi) = \frac{1}{2}\sigma(e^+e^- \to \pi^+\pi^- J/\psi)$
  - $\sigma(e^+e^- \to \pi^+\pi^- J/\psi)$ can be got from [1]

[1] Z. Q. Liu *et al.* (Belle Collaboration), Phys. Rev. Lett. **110**, 252002 (2013)

Potential background

- Non J/ψ background. This can be estimated by J/ψ sideband
- $e^+e^- \to \gamma_{\rm ISR} J/\psi$
  - This cross section can be calculated theoretically
- $e^+e^- \to \gamma_{\rm ISR} \pi^0\pi^0 J/\psi$
  - $\sigma(e^+e^- \to \pi^0\pi^0 J/\psi) = \frac{1}{2}\sigma(e^+e^- \to \pi^+\pi^- J/\psi)$
  - $\sigma(e^+e^- \to \pi^+\pi^- J/\psi)$ can be got from [1]
- $e^+e^- \to \gamma_{\rm ISR} \eta J/\psi$
  - $\sigma(e^+e^- \to \eta J/\psi)$ can be got from [2]

[1] Z. Q. Liu *et al.* (Belle Collaboration), Phys. Rev. Lett. **110**, 252002 (2013)

[2] X. L. Wang *et al.* (Belle Collaboration), Phys. Rev. D **87**, 051101 (2013).

Potential background

- Non J/ψ background. This can be estimated by J/ψ sideband
- $e^+e^- \to \gamma_{\rm ISR} J/\psi$
  - This cross section can be calculated theoretically
- $e^+e^- \to \gamma_{\rm ISR} \pi^0\pi^0 J/\psi$
  - $\sigma(e^+e^- \to \pi^0\pi^0 J/\psi) = \frac{1}{2}\sigma(e^+e^- \to \pi^+\pi^- J/\psi)$
  - $\sigma(e^+e^- \to \pi^+\pi^- J/\psi)$ can be got from [1]
- $e^+e^- \to \gamma_{\rm ISR} \eta J/\psi$
  - $\sigma(e^+e^- \to \eta J/\psi)$ can be got from [2]
- $e^+e^- \to \gamma_{\rm ISR} \psi(2S)$ at high mass region

[1] Z. Q. Liu *et al.* (Belle Collaboration), Phys. Rev. Lett. **110**, 252002 (2013)

[2] X. L. Wang *et al.* (Belle Collaboration), Phys. Rev. D **87**, 051101 (2013).

Efficiency

There is only one ISR photon generated in EVTGEN. The efficiency will be over-estimated. We need to correct this.

- PHOKHARA can be used to generate $e^+e^- \to \gamma_{ISR}\eta J/\psi$ with one or two ISR photons.
- EVTGEN can also generate $e^+e^- \to \gamma_{ISR}\eta J/\psi$
- The difference is used to correct the ISR effect

The process $\psi(2S) \to \gamma\chi_{cJ} \to \gamma\gamma J/\psi$ is dominated by "E1" transition, with some mixing of "M2" and "E3". The photon angular distribution is given in [1].
This is also considered by assuming that all ISR photons is emitted from initial electrons.

[1] Karl G *et al.* Phys. Rev. D **13**, 1203 (1976)

Efficiency curve and $\gamma\gamma J/\psi$ mass

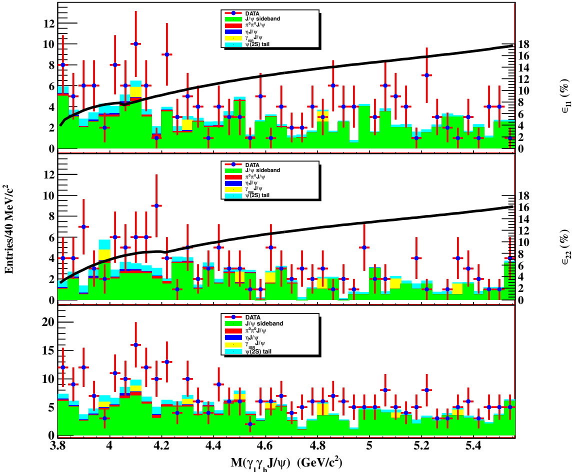

Figure: Invariant mass distributions of $\gamma\chi_{cJ}$ candidates. Shown from top to bottom are $\gamma\chi_{c1}$, $\gamma\chi_{c2}$, and their sum.

$\psi(2S) \to \gamma\chi_{cJ}$ branching fractions

$\psi(2S)$ signal region: $3.65 < M(\gamma_l\gamma_h J/\psi) < 3.72\ \mathrm{GeV}/c^2$.

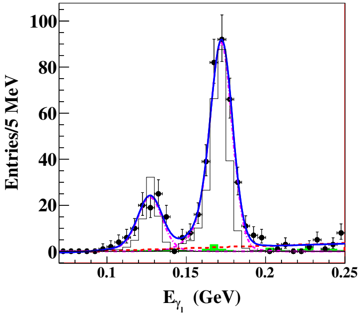

Figure: Energy distributions of the low energy photon in the $\gamma_l\gamma_h J/\psi$ CM system for events in the $\psi(2S)$ mass region.

The fit gives 340 ± 20 χ_{c1} and 97 ± 12 χ_{c2} signal events.

- $\sigma[e^+e^- \to \gamma_{\mathrm{ISR}}\psi(2S)] = (14.25 \pm 0.26)$ pb
- $\mathcal{L} = 980$ fb^{-1}
- $\epsilon_{\chi_{c1}} = 1.4\%$, $\epsilon_{\chi_{c2}} = 0.7\%$

$\mathcal{B}[\psi(2S) \to \gamma\chi_{c1} \to \gamma\gamma J/\psi) = (2.92 \pm 0.19)\%$

$\mathcal{B}[\psi(2S) \to \gamma\chi_{c2} \to \gamma\gamma J/\psi) = (1.65 \pm 0.21)\%$

PDG14 gives 2.93 ± 0.15 and 1.52 ± 0.15

High mass region study

The high mass region: $M(\gamma\gamma J/\psi) \in [3.8,\ 5.56]\ \mathrm{GeV}/c^2$

There is no obvious signals, upper limits are given.

Cross section upper limit

We first construct the likelihood function $L(N^{\chi_{c1}}, N^{\chi_{c2}})$ for the number of produced events.
Using $L(N^{\chi_{c1}}, N^{\chi_{c2}})$, upper limit of $N^{\chi_{c1}}$ and $N^{\chi_{c2}}$ at 90% C.L. can be got. And then the upper limit of $\sigma(e^+e^- \to \gamma\chi_{cJ})$.

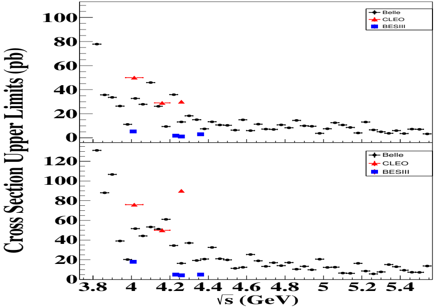

Figure: Measured upper limits on the $e^+e^- \to \gamma\chi_{cJ}$ cross sections at the 90% C.L. for χ_{c1} (top) and χ_{c2} (bottom).

Transition rate of charmonium to $\gamma\chi_{cJ}$

We can fit the mass spectrum of $\gamma\gamma J/\psi$ to get transition rate of the vector charmonium to $\gamma\chi_{cJ}$.

- One Breit-Wigner function as the signal and a linear function as the background
- The mass and total width are fixed
- $\Gamma_{ee} \times \mathcal{B}(R \to \gamma\chi_{cJ})$ is scanned to obtain the p.d.f.

Table: Upper limits on $\Gamma_{ee} \times \mathcal{B}$ at the 90% C.L.

	χ_{c1} (eV)	χ_{c2} (eV)
$\Gamma_{ee}[\psi(4040)] \times \mathcal{B}[\psi(4040) \to \gamma\chi_{cJ}]$	2.9	4.6
$\Gamma_{ee}[\psi(4160)] \times \mathcal{B}[\psi(4160) \to \gamma\chi_{cJ}]$	2.2	6.1
$\Gamma_{ee}[\psi(4415)] \times \mathcal{B}[\psi(4415) \to \gamma\chi_{cJ}]$	0.47	2.3
$\Gamma_{ee}[Y(4260)] \times \mathcal{B}[Y(4260) \to \gamma\chi_{cJ}]$	1.4	4.0
$\Gamma_{ee}[Y(4360)] \times \mathcal{B}[Y(4360) \to \gamma\chi_{cJ}]$	0.57	1.9
$\Gamma_{ee}[Y(4660)] \times \mathcal{B}[Y(4660) \to \gamma\chi_{cJ}]$	0.45	2.1

Upper limits on branching fractions

Taking $\Gamma_{ee}[\psi(4040)]$ and $\Gamma_{ee}[\psi(4415)]$ from the world average values and $\Gamma_{ee}[\psi(4160)]$ from the BES II measurement.

Table: Upper limits on branching fractions $\mathcal{B}(R \to \gamma\chi_{cJ})$ at the 90% C.L.

Resonance	$\gamma\chi_{c1}$ (10^{-3})	$\gamma\chi_{c2}$ (10^{-3})
$\psi(4040)$	3.4	5.5
$\psi(4160)$	6.1	16.2
$\psi(4415)$	0.83	3.9

Upper limits on branching fractions ratio

Taking $\Gamma_{ee}[Y(4260)] \times \mathcal{B}[Y(4260) \to \pi^+\pi^- J/\psi] = (6.4 \pm 0.8 \pm 0.6)$ eV or $(20.5 \pm 1.4 \pm 2.0)$ eV [1]

$\Gamma_{ee}[Y(4360)] \times \mathcal{B}[Y(4360) \to \pi^+\pi^- \psi(2S)] = (10.4 \pm 1.7 \pm 1.4)$ eV or $(11.8 \pm 1.8 \pm 1.4)$ eV [2]

$\Gamma_{ee}[Y(4660)] \times \mathcal{B}[Y(4660) \to \pi^+\pi^- \psi(2S)] = (3.0 \pm 0.9 \pm 0.3)$ eV or $(7.6 \pm 1.8 \pm 0.8)$ eV [2]

Table: Upper limits on branching fraction ratios at the 90% C.L.

Resonance	$\gamma\chi_{c1}$	$\gamma\chi_{c2}$
$\frac{\mathcal{B}[Y(4260)\to\gamma\chi_{cJ}]}{\mathcal{B}[Y(4260)\to\pi^+\pi^- J/\psi]}$	0.3 or 0.07	0.7 or 0.2
$\frac{\mathcal{B}[Y(4360)\to\gamma\chi_{cJ}]}{\mathcal{B}[Y(4360)\to\pi^+\pi^- \psi(2S)]}$	0.06 or 0.05	0.2 or 0.2
$\frac{\mathcal{B}[Y(4660)\to\gamma\chi_{c1}]}{\mathcal{B}[Y(4660)\to\pi^+\pi^- \psi(2S)]}$	0.2 or 0.07	0.9 or 0.3

[1] Z. Q. Liu *et al.* (Belle Collaboration), Phys. Rev. Lett. **110**, 252002 (2013)

[2] X. L. Wang *et al.* (Belle Collaboration), Phys. Rev. Lett. **99**, 142002 (2007)

Systematic uncertainty

- Tracking efficiency: 0.35% per track
- particle identification: 1.9%
- J/ψ and χ_{cJ} mass: 1.0% and 1.3%
  - Estimate with $\psi(2S) \to \gamma\chi_{cJ}$
- Generator
  - Corrected with $e^+e^- \to \eta J/\psi$, The difference 9.0% between measured $\mathcal{B}$ and PDG14 is taken
  - EVTGEN: 1.0%
  - Statistical error of the MC samples: 2.0%
- Luminosity: 1.4%
- Trigger: 2%
- Branching fractions of the intermediate states: 4.5%

Assuming that all these systematic error sources are independent, the total systematic error is 13.4%.

Summary

- The process $e^+e^- \to \gamma_{ISR}\gamma\chi_{cJ}$ is studied using full Belle data sample
- There is no obvious $\gamma\chi_{cJ}$ signal at high mass region
- The analysis is validated with branching fraction of $\mathcal{B}[\psi(2S) \to \gamma\chi_{cJ} \to \gamma\gamma J/\psi)]$
- Cross section upper limit of $e^+e^- \to \gamma\chi_{cJ}$ is set at 90% C.L. between $\sqrt{s} = 3.8$ to $5.56~\mathrm{GeV}$
- Upper limits on the decay rate of the vector charmonium [$\psi(4040)$, $\psi(4160)$, and $\psi(4415)$] and charmoniumlike [$Y(4260)$, $Y(4360)$, and $Y(4660)$] states to $\gamma\chi_{cJ}$ is also set at 90% C.L.

Thank You!

Backup

Event selection

- Two good charged tracks with zero net charge
  - $P_T > 0.1\ \mathrm{GeV/c}$
  - $|dr| < 0.5$ cm, $|dz| < 5.0$ cm for charged tracks
- Muon identification is required
  - One track should satisfy $\mathcal{R}_\mu = \frac{\mathcal{L}_\mu}{\mathcal{L}_\mu + \mathcal{L}_\pi} > 0.95$
  - If $\mathcal{R}_\mu = 0$ for one track, $|\cos\theta_\mu| < 0.75$ is required for each track
- A photon candidate does not match any charged tracks
  - Photons with $E_\gamma > 3\ \mathrm{GeV}$ in e^+e^- CM will be labeled as ISR photon (Excluded)
  - $E_\gamma > 0.25\ \mathrm{GeV}$ in lab. system
  - Two highest energy photons in the laboratory system
- Reject $\eta(\pi^0)J/\psi$ events
  - $M(\gamma\gamma)$ are not in the η mass region $[0.50,\ 0.58]\ \mathrm{GeV}/c^2$
  - $M(\gamma\gamma) > 0.20\ \mathrm{GeV}/c^2$ to reject π^0 and other low invariant mass events

Invariant mass of $\gamma_l \gamma_h J/\psi$

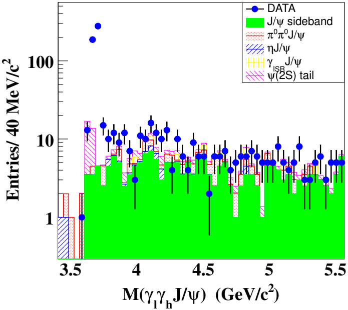

Figure: Invariant mass distribution of $\gamma_l \gamma_h J/\psi$. The background from the tail of the $\psi(2S)$ is plotted only for $M(\gamma_l \gamma_h J/\psi) > 3.75\ \mathrm{GeV}/c^2$ and $M(\gamma_l \gamma_h J/\psi) < 3.65\ \mathrm{GeV}/c^2$.

Cross section upper limit

Maximum likelihood is used to get the upper limits.

The numbers of the expected signal events, $\nu^{\chi_{c1}}$ and $\nu^{\chi_{c2}}$

$$\begin{pmatrix} \nu^{\chi_{c1}} \\ \nu^{\chi_{c2}} \end{pmatrix} = \begin{pmatrix} \epsilon_{11} & \epsilon_{21} \\ \epsilon_{12} & \epsilon_{22} \end{pmatrix} \begin{pmatrix} N^{\chi_{c1}} \times \mathcal{B}(\chi_{c1} \to \gamma J/\psi) \times \mathcal{B}(J/\psi \to \mu^+\mu^-) \\ N^{\chi_{c2}} \times \mathcal{B}(\chi_{c2} \to \gamma J/\psi) \times \mathcal{B}(J/\psi \to \mu^+\mu^-) \end{pmatrix}$$

The numbers of expected events

$$\begin{pmatrix} \mu^{\chi_{c1}} \\ \mu^{\chi_{c2}} \end{pmatrix} = \begin{pmatrix} \nu^{\chi_{c1}} \\ \nu^{\chi_{c2}} \end{pmatrix} + \begin{pmatrix} n^{\chi_{c1}}_{\mathrm{bkg}} \\ n^{\chi_{c2}}_{\mathrm{bkg}} \end{pmatrix},$$

The probability of observing $(n^{\chi_{c1}}_{\mathrm{obs}},\ n^{\chi_{c2}}_{\mathrm{obs}})$

$$p(N^{\chi_{c1}}, N^{\chi_{c2}}) = \frac{(\mu^{\chi_{c1}})^{n^{\chi_{c1}}_{\mathrm{obs}}} e^{-\mu^{\chi_{c1}}}}{n^{\chi_{c1}}_{\mathrm{obs}}!} \frac{(\mu^{\chi_{c2}})^{n^{\chi_{c2}}_{\mathrm{obs}}} e^{-\mu^{\chi_{c2}}}}{n^{\chi_{c2}}_{\mathrm{obs}}!}$$

Considering the uncertainty in the background estimation and systematic error

$$L(N^{\chi_{c1}}, N^{\chi_{c2}}) = \sum_{k,l,m,n} p(N^{\chi_{c1}}, N^{\chi_{c2}}) = \sum_{k,l,m,n} \frac{(\mu^{\chi_{c1}}_{k,l})^{n^{\chi_{c1}}_{\mathrm{obs}}} e^{-\mu^{\chi_{c1}}_{k,l}}}{n^{\chi_{c1}}_{\mathrm{obs}}!} \frac{(\mu^{\chi_{c2}}_{m,n})^{n^{\chi_{c2}}_{\mathrm{obs}}} e^{-\mu^{\chi_{c2}}_{m,n}}}{n^{\chi_{c2}}_{\mathrm{obs}}!}$$